Table 2 Summary of optimum results, stacking sequence of symmetric 24-ply laminated walls

Stacking sequence	Reference horizontal and vertical wall, deg	Optimum horizontal wall, deg	Optimum vertical wall, deg
θ_1	Outer ply, 0	15	15
θ_2	0	−15	−15
θ_3	0	0	−15
θ_4	0	0	−15
θ_5	15	45	30
θ_6	−15	−45	−30
θ_7	15	45	30
θ_8	−15	−45	−30
θ_9	45	0	0
θ_{10}	−45	0	0
θ_{11}	45	30	15
θ_{12}	Midplane, −45	−30	−15

after optimization represents a compromise between the conflicting requirements of reduced elastic twist and reduced transverse displacements. This is observed by noting the inclusion of ±30-deg plies in both the horizontal and the vertical walls. The reductions in all of the tip displacements are attributable to the improved ply-stacking sequence and the increased thickness of the airfoil caused by larger chords, which in turn increases the box beam height.

Concluding Remarks

The results of a multiple design point optimization procedure for design of high-speed proprotors were presented. The procedure was based on multilevel decomposition and a multiobjective formulation that used the K–S function technique. Aerodynamic performance was the objective of the upper level and the structural response was improved at the lower level. Optimization was performed simultaneously to include design criteria from high-speed cruise, hover, and takeoff. A nonlinear programming technique was used at the upper level and a simulated annealing algorithm was used for the discrete optimization problem at the lower level. The optimum results were compared with a reference rotor. The following are some important observations:

1) The multilevel optimization procedure significantly improves the aerodynamic and structural response of the high-speed proprotor blade at all three flight conditions.

2) Optimum planform distributions represent compromises between the conflicting requirements of the three flight conditions. At locations near the root and the tip, the optimizer is driven by the geometric constraints imposed on the problem.

3) The simulated annealing algorithm successfully minimizes the tip displacements by altering the composite plate stacking sequences in the horizontal and vertical walls. The optimum stacking sequence represents a compromise between reduced elastic twist and reduced transverse deformation. This is manifested through the selection of ±30-deg plies in both the horizontal and the vertical walls.

4) A combination of improved stacking sequence and larger chord values leads to reduced elastic deformation in the optimum configurations.

Acknowledgment

The authors acknowledge the support of this research through a grant from NASA Ames Research Center, Grant NCC2-795, Technical Monitors were John F. Madden III and Sesi Kottapalli.

References

[1]Chattopadhyay, A., McCarthy, T. R., and Seeley, C. E., "A Decomposition Based Optimization Procedure for High Speed Prop-Rotors Using Composite Tailoring and Simulated Annealing," *Journal of Aircraft*, Vol. 32, No. 5, 1995, pp. 1026–1033.

[2]Dadone, L., Liu, J., Wilkerson J., and Acree, C. W., "Proprotor Design Issues for High Speed Tiltrotors," *Proceedings of the 50th Annual Forum of the American Helicopter Society*, American Helicopter Society, Washington, DC, 1994.

[3]Chattopadhyay, A., and Seeley, C. E., "A Simulated Annealing Technique for Multiobjective Optimization of Intelligent Structures," *Journal of Smart Materials and Structures*, Vol. 3, June 1994, pp. 98–106.

[4]Chattopadhyay, A., McCarthy, T. R., and Seeley, C. E., "A Multiple Design Point Optimization of High Speed Proprotors," *Proceedings of the 20th European Rotorcraft Forum* (Amsterdam, The Netherlands), 1994 (Paper 47).

[5]Tsai, S. W., and Wu, E. M., "A General Theory of Strength for Anisotropic Materials," *Journal of Composite Materials*, Vol. 5, Jan. 1971, pp. 58–80.

[6]Lamon, S., "XV-15 Advanced Technology Blades, Ultimate Stress Analysis," Boeing Rept. D210-12345-1, 1985.

[7]Agarwal, B. D., and Broutman, L. J., *Analysis and Performance of Fiber Composites*, Wiley, New York, 1990.

[8]Haftka, R. T., Gürdal, Z., and Kamat, M. P., *Elements of Structural Optimization*, Kluwer, Dordrecht, The Netherlands, 1990.

Identification of Lateral–Directional Behavior in Stall from Flight Data

J. Singh* and R. V. Jategaonkar†
DLR, German Aerospace Research Establishment, D-38108 Brunswick, Germany

Introduction

AERODYNAMICS associated with aircraft flight in stall and poststall regimes are of increasing interest. Computational fluid dynamic methods[1,2] and a number of semiempirical models[3,4] have resulted in a significantly improved modeling of unsteady stalled flow. Much of the research work is, however, based on wind-tunnel data from unsteady airfoil tests and only a few applications to identification from flight data have been reported.[5,6] Moreover, analysis in the stall and poststall region is more or less confined only to the longitudinal dynamics. Recently, based on a state–space representation of unsteady aerodynamics at high angle of attack,[7] the problem of stall identification from flight data pertaining to the longitudinal dynamics has been addressed.[8] Flight analysts have, however, encountered cases in the past where an aircraft in stall is known to have exhibited large excursions in the lateral–directional motion. This behavior is attributed mainly to the significant sideforce and yawing moments generated because of formation and shedding of the forebody vortices.[9,10]

In this Note, the stall model is extended to asymmetric unsteady flow phenomenon and applied to identify, from flight data, the lateral–directional behavior of the C-160 aircraft. Both dynamic and quasisteady stall maneuvers are analyzed. It is observed that different flow separation points on the left and the right wing surfaces adequately characterize the pronounced variations in the lateral–directional motion of the quasisteady stall.

Stall Modeling

The trailing-edge stall is a dominating phenomenon on wings having sufficient thickness ($t/\bar{c} > 0.15$; where t repre-

Received July 7, 1995; revision received Nov. 8, 1995; accepted for publication Dec. 4, 1995.

*Guest Scientist, Institute of Flight Mechanics. Member AIAA.
†Senior Scientist, Institute of Flight Mechanics. Member AIAA.

sents wing thickness and $\bar{c}$ the wing mean aerodynamic chord), and undergoing a relatively slow variation in the angle of attack ($\dot{\alpha} < 0.02V/\bar{c}$; where $\dot{\alpha}$ is the rate of change of angle of attack and V is the freestream velocity). The associated loss of circulation because of trailing-edge separation introduces a nonlinear behavior in the lift coefficient C_L and the incremental drag coefficient ΔC_D, which can be approximated using Kirchhoff's theory of flow separation[4]:

$$C_L = C_{L\alpha}[(1 + \sqrt{x})/2]^2 \sin \alpha \tag{1a}$$

$$\Delta C_D = C_{L\alpha}[(1 - \sqrt{x})/2]^2 \sin \alpha \tan \alpha \tag{1b}$$

where $C_{L\alpha}$ is the lift curve slope and $x \in [0, 1]$ is a dynamical variable describing the location of the flow separation point along the chord on the upper surface of the wing; $x = 1$ and $x = 0$ correspond to the attached and fully separated flow, respectively. The unsteady stalled flow conditions can be conveniently described using a single ordinary differential equation[7,8]:

$$\tau_1 \frac{dx}{dt} + x = x_0(\alpha - \tau_2 \dot{\alpha}) \tag{2}$$

where τ_1 and τ_2 are the time constants representing the transient and the quasisteady aerodynamic effects, respectively. The steady flow separation point x_0 may be determined from static wind-tunnel tests, or can also be identified from flight tests using the approximation[8]:

$$x_0(\alpha) = \tfrac{1}{2}\{1 - \tanh[a_1(\alpha - \alpha^*)]\} \tag{3}$$

where the parameter a_1 defines the static stall characteristics of the airfoil, and α^* defines the breakpoint corresponding to $x_0 = 0.5$.

In Ref. 8, Eqs. (1–3) are applied to the C-160 flight data in the high-lift region. A good match between the model output and the measured data for pitch rate, angle of attack, and normal acceleration shows the ability of the model to satisfactorily identify the longitudinal behavior in stall. However, the same cannot be stated for the lateral case where poor simulation quality, specifically in quasisteady stall approach, for the lateral–directional time histories is observed (Fig. 1, discussed later in the text). The C-160 aircraft flight data reveal that the quasisteady stall is accompanied by an uncommanded left roll off, which is apparently because of the unequal lift caused by the different flow separation behavior on the left and the right wing.

Asymmetric Aerodynamic Modeling

To account for the asymmetric flow separation on the two wing panels, the rolling and yawing moment coefficients are suitably modified as follows to account for the additional moments arising from the different flow separation points:

$$C_l = C_{l0} + C_{l\beta}\beta + C_{lp}p^* + C_{lr}r^* + C_{l\delta a}\delta_a + C_{l\delta r}\delta_r + (1/2b)[(C_N)_L - (C_N)_R]\Delta y \tag{4a}$$

$$C_n = C_{n0} + C_{n\beta}\beta + C_{np}p^* + C_{nr}r^* + C_{n\delta a}\delta_a + C_{n\delta r}\delta_r + (1/2b)[(C_c)_L - (C_c)_R]\Delta y \tag{4b}$$

where b is the wingspan; Δy represents the moment lever arm equal to half the wingspan; δ_a and δ_r denote the aileron and rudder deflections, respectively; β is the angle of sideslip; p^* and r^* are the normalized roll and yaw rates, respectively; and $C_{l(\cdot)}$ and $C_{n(\cdot)}$ are the aerodynamic derivatives. The suffixes L and R represent parameters for the left and the right wing, respectively. The normal force coefficient C_N and the chord force coefficient C_c can be obtained by resolving the forces on the airfoil as follows:

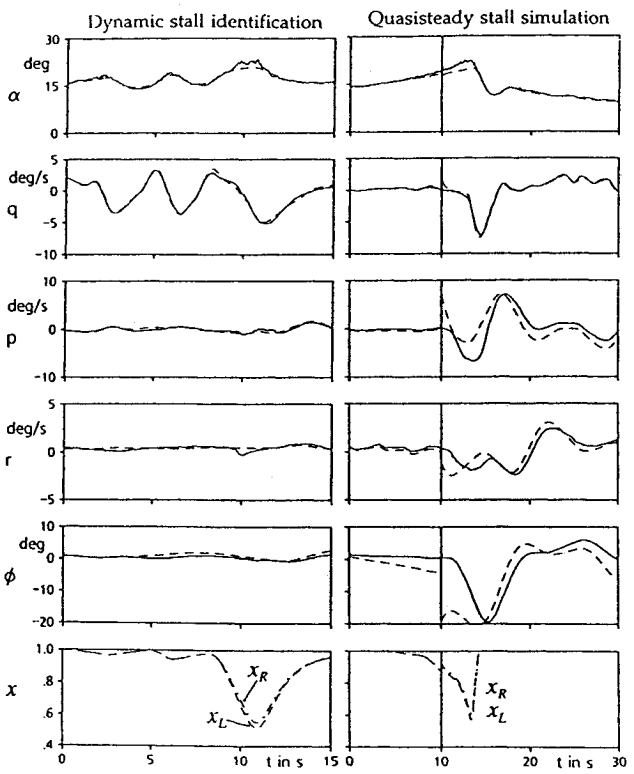

Fig. 1 C-160 dynamic stall identification and quasisteady stall simulation: —, flight measured; ---, estimated.

$$(C_N)_{L,R} = (C_L)_{L,R} \cos \alpha + (C_D)_{L,R} \sin \alpha \tag{5a}$$

$$(C_c)_{L,R} = C_{L\alpha}\sqrt{x_{L,R}} \sin^2\alpha \tag{5b}$$

Equation (4), incorporating the lift and drag differentials, leads not only to a parsimonious model, but is also based on the physical interpretation of the force/moment phenomenon. This approach appears to be preferable compared to the other approach of modeling the rolling and yawing moments because of asymmetric unsteady flow through additional aerodynamic derivatives.

Stall Identification

Equations (2) and (3) describing flow separation point, and Eqs. (4) and (5) describing the asymmetric aerodynamic modeling, are used in conjunction with the longitudinal model to identify the C-160 flight data in stall.[8] The unsteady model equations are implemented into the 6-degree-of-freedom model formulated in Ref. 11. Maximum-likelihood identification algorithm for nonlinear systems[12] is used to identify the stall parameters a_1 and α^* for the left and right wing panels, and the time constants τ_1 and τ_2. All other parameters of the basic aerodynamic model pertaining to the attached flow conditions are kept fixed during estimation.[11]

Plots on the left side of Fig. 1 for the dynamic stall identification show an acceptable match between the estimated and the flight measured responses for the longitudinal variables, the pitch rate q, and the angle of attack α, as well as lateral variables, the roll rate p, the yaw rate r, and the bank angle ϕ. The variations in the lateral–directional motion are observed to be small. Also shown is the estimated time variation of x_L and x_R, which defines the location of separation points on the left and the right wing, respectively. It can be seen that as the angle of attack increases, the trailing-edge separation progresses towards the leading edge, showing a maximum flow

separation of about 50% at an angle of attack $\alpha \approx 23$ deg. Furthermore, the marginal difference between x_L and x_R signifies that the flow separation on the two wing panels is more or less symmetric during the dynamic stall maneuver.

Plots on the right side of Fig. 1 depict quasisteady stall simulation carried out by keeping the stall parameter values identified from the dynamic stall maneuvers fixed and adjusting only the initial conditions to match the new flight condition. Results indicate discernible mismatch in lateral variables p, r, and ϕ responses, whereas flight variables q and α are fairly well simulated. This inability of the dynamic stall model to adequately predict the lateral motion of the quasisteady stall is attributed to the asymmetric effects that are insignificant in the dynamic stall maneuver, but have a very strong influence on the lateral–directional behavior during quasisteady stall maneuver. Note that to minimize the errors associated with the identification of long time segments, the 70-s time segment of the quasisteady stall is split into two. Figure 1 and the subsequent plots, however, depict only that portion where significant variations in the flight variables are observed.

To account for the aforementioned discrepancies, the asymmetric unsteady stall model proposed in this Note is applied to analyze the quasisteady stall maneuver. The stall parameters

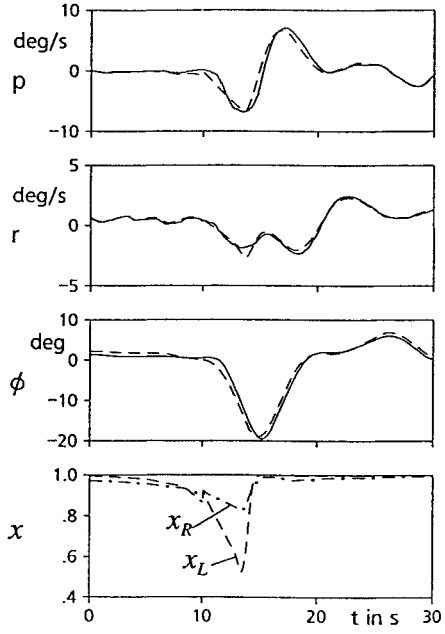

Fig. 2 C-160 quasisteady stall identification: —, flight measured; ---, estimated.

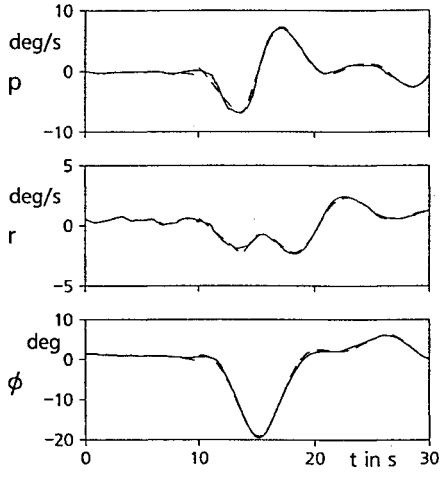

Fig. 3 Influence of cross and cross-coupling derivatives at high α: —, flight measured; ---, estimated.

a_1 and α^* for the left and the right wings and the time constant τ_2 are estimated separately. The capability of the present formulation to satisfactorily identify the lateral–directional motion of the quasisteady stall is evident from the comparison of the estimated and flight measured responses shown in Fig. 2. The asymmetry in flow separation is clearly observed from the plots of the separation points x_L and x_R. Such an effect could possibly be because of the two engines equipped with four-bladed propellers rotating in the same direction and influencing the flow separation in an asymmetric way. Furthermore, the estimated values of the stall parameters differ significantly from the values identified from the dynamic stall maneuvers.

Although the basic phenomenon of asymmetric flow separation is well captured with the present formulation, minor discrepancies are observed in the time history match shown in Fig. 2. It is known from literature that cross and cross-coupling derivatives can have significant influence on aircraft motion at high angles of attack.[10] A judicious inclusion of such derivatives into the model equations can result in a better prediction of the stall behavior. Figure 3 shows an improved match with the cross derivatives C_{l_r} and C_{n_p}, and cross-coupling derivatives C_{l_q} and C_{n_q} included into the estimation model. However, more data need to be analyzed to positively conclude that the inclusion of these additional derivatives actually improves the predictive capabilities of the model.

Conclusions

The unsteady stall model is extended to identify the lateral–directional behavior in stall from flight data. Additional rolling and yawing moments arising from the differential lift and drag because of unsymmetric flow separation on the left and the right wing are included in the estimation model in a simple, but physically representative, way. The results demonstrate the model's ability to identify the longitudinal and lateral dynamics in stall. Analysis of the C-160 flight data in the high-lift region indicates that unlike in dynamic stall, the flow separation behavior in the quasisteady stall is highly asymmetric, producing significant roll and yaw without any input from the pilot. Furthermore, it appears difficult to arrive at a single stall model that can adequately predict both the quasisteady and the dynamic stall behavior of the aircraft.

Acknowledgment

This work was carried out during the tenure of postdoctoral fellowship awarded by the Humboldt Foundation, Bonn, Germany, to J. Singh.

References

[1]Shamroth, S. J., "Calculation of Steady and Unsteady Airfoil Flow Fields via the Navier Stokes Equations," NASA CR-3899, 1985.

[2]Tuncer, I., Wu, J., and Wang, C., "Theoretical and Numerical Studies of Oscillating Airfoils," AIAA Paper 89-0021, Jan. 1989.

[3]Gangwani, S. T., "Prediction of Dynamic Stall and Unsteady Airloads for Rotor Blades," *Journal of the American Helicopter Society*, Vol. 27, No. 4, 1982, pp. 57–64.

[4]Leishman, J. G., and Beddoes, T. S., "A Semi-Empirical Model for Dynamic Stall," *Journal of the American Helicopter Society*, Vol. 34, No. 3, 1989, pp. 3–17.

[5]Wilson, D. B., and Winters, C. P., "F-15A Approach-to-Stall/Stall/Post-Stall Evaluation," Air Force Flight Test Center, AFFTC TR-75-32, Edwards AFB, CA, Jan. 1976.

[6]Vincent, J. H., Gupta, N. K., and Hall, W. E., "Recent Results in Parameter Identification for High Angle of Attack Stall Regimes," AIAA Paper 79-1640, Aug. 1979.

[7]Goman, M., and Khrabrov, A., "State-Space Representation of Aerodynamic Characteristics of an Aircraft at High Angles of Attack," *Journal of Aircraft*, Vol. 31, No. 5, 1994, pp. 1109–1115.

[8]Fischenberg, D., "Identification of an Unsteady Aerodynamic Stall Model from Flight Test Data," AIAA Paper 95-3438, Aug. 1995.

[9]Skow, A. M., Titiriga, A., and Moore, W. A., "Forebody/Wing Vortex Interactions and Their Influence on Departure and Spin Resistance," CP-247, AGARD, Oct. 1978, pp. 6-1–6-26.

[10]Orlik-Rückemann, K. J., "Aerodynamic Aspects of Aircraft Dynamics at High Angles of Attack," *Journal of Aircraft*, Vol. 20, No. 9, 1983, pp. 737–751.

[11]Jategaonkar, R. V., Mönnich, W., Fischenberg, D., and Krag, B., "Data Gathering for C-160 Transall Flight Simulator, Part 1: Math Model and Aerodynamic Data Base," DLR-IB 111-93/37, Brunswick, Germany, May 1993.

[12]Jategaonkar, R. V., and Plaetschke, E., "Maximum Likelihood Parameter Estimation from Flight Test Data for General Non-Linear Systems," DFVLR-FB 83-14, Brunswick, Germany, March 1983.

Airfoil Design Utilizing Parallel Processors

Stephen C. Brawley* and Garth V. Hobson†
U.S. Naval Postgraduate School, Monterey, California 93943

Introduction

AN aerodynamic design scheme using parallel processors has been developed that significantly decreases the processing time required to optimize a desired performance. The parallel optimization scheme, when coupled with a flow solver, evaluates the aerodynamic performance of numerous geometries simultaneously. A test case was conducted utilizing the parallel optimization scheme and a similar sequential optimization scheme to design an airfoil to match the pressure distribution corresponding to a known shape. This design application demonstrates the practicality and versatility of aerodynamic design via optimization using parallel processors.

Computational fluid dynamics (CFD) has become a valuable engineering tool in both aerodynamic analysis and design. Airfoil optimization uses multivariable calculus to minimize an objective function selected by the designer. If the objective function is continuous, which is usually the case in airfoil design, the desired performance of the airfoil is optimized as the objective function is reduced.

Optimization methods for airfoil design have many advantages, including the flexibility of the designer to choose various design performance criteria and to use different types of flow solvers. However, their main disadvantage is the amount of computer processing time required for the design criteria to be optimized. Flowfield calculations over various geometries of airfoils that evaluate their aerodynamic performances constitute the vast majority of the computer time required.

To significantly speed up the design, the required processing time must be reduced. An investigation into gradient-based optimization schemes reveals that airfoil design can be treated as a parallel problem and can take advantage of the capabilities of parallel supercomputers. Parallel processors are used to conduct multiple CFD solutions for different airfoil geometries simultaneously to reduce the time required for airfoil design via optimization.

Presented as Paper 95-0125 at the AIAA 33rd Aerospace Sciences Meeting and Exhibit, Reno, NV, Jan. 9–12, 1995; received Feb. 19, 1995; revision received Oct. 1, 1995; accepted for publication Oct. 16, 1995.

*Adjunct Professor, Department of Aeronautics and Astronautics. Member AIAA.

†Associate Professor, Department of Aeronautics and Astronautics. Member AIAA.

Quasi-Newton Optimization Using Parallel Processors

An objective function appropriate for airfoil design is based upon the aerodynamic performance of the airfoil. Numerous evaluations of the objective function f are necessary for the gradient calculations and for line searches to locate a minimum. Since each objective function evaluation requires a CFD solution, the vast majority of computational time needed to design an airfoil is spent calculating the flowfield around various airfoil geometries.

Kennelly[1] developed the optimization routine QNMDIF based upon a quasi-Newton method and used the routine in airfoil design. In this research, parallel processors are used to simultaneously calculate the flowfields over multiple airfoil geometries for the estimation of the gradient vectors and in directional searches for minimum objective functions. Conducting the gradient calculations and line searches in parallel greatly increases the speed and efficiency of the design procedure.

The parallel quasi-Newton optimization routine, PARQNM, assigns multiple processors to simultaneously calculate objective functions with different sets of design variables. For a second-order-accurate estimation of each component of the gradient, two function evaluations are required. For example, the first gradient component is estimated from the central-differencing calculation

$$\frac{\partial f}{\partial x_1} = \frac{f(x_1 + \Delta x_1, x_2, \ldots, x_n)}{2\Delta x_1} - \frac{f(x_1 - \Delta x_1, x_2, \ldots, x_n)}{2\Delta x_1} \quad (1)$$

For n design variables, $2n$ processors are used in PARQNM to calculate all forward- and backward-difference function evaluations in parallel for the estimation of the gradient vector.

The method of gradient calculation used in PARQNM has several advantages over the method used in the sequential quasi-Newton routine QNMDIF. Most importantly, all function evaluations are done in parallel instead of sequentially. Also, the central-difference estimation of each gradient component used in the parallel routine is more accurate than the forward-difference estimation used in QNMDIF. In QNMDIF, if the forward-difference estimation of the gradient fails to provide a direction that reduces the objective function in a line search, valuable processing time will be wasted before computing the gradient derivatives based upon a central-difference approximation.

A parallel line search was developed that minimizes a multivariable objective function more efficiently and many times faster than the line search used in the sequential optimization routine. After the direction of search P is calculated based upon the gradient vector, the new set of design variables X becomes a function of a scalar q as shown in Eq. (2):

$$\boldsymbol{X}^{k+1} = \boldsymbol{X}^k + q\boldsymbol{P}^k \quad (2)$$

Different values of q are assigned to the processors in equal intervals between its minimum and maximum values selected by the designer. Each processor then simultaneously computes the objective function for a unique set of design variables. The new set of design variables corresponding to the minimum objective function is then sent to all processors in a global message.

The parallel line search conducts all expensive function evaluations in parallel, unlike the sequential version that requires numerous function evaluations calculated sequentially using parabolic interpolation. Also, the parallel line search helps protect against convergence to a local minimum instead of a global minimum because of more function evaluations along the line of search.